Journal of Biomechanics 46 (2013) 2220–2227

Contents lists available at ScienceDirect

Journal of Biomechanics

journal homepage: www.elsevier.com/locate/jbiomech
www.JBiomech.com

Estimation of external contact loads using an inverse dynamics and optimization approach: General method and application to sit-to-stand maneuvers

T. Robert [a,*], J. Causse [a,b], G. Monnier [a,c]

[a] Université de Lyon, F-69622, Lyon, IFSTTAR, LBMC, UMR_T9406, Université Lyon 1, France
[b] PSA Peugeot-Citroen, France
[c] In-Motion, France

ARTICLE INFO

Article history:
Accepted 23 June 2013

Keywords:
Inverse dynamics
Underdetermined problem
External contact loads
Joint loads
Optimization
Sit-to-stand

ABSTRACT

This paper presents a general method to estimate unmeasured external contact loads (ECLs) acting on a system whose kinematics and inertial properties are known. This method is dedicated to underdetermined problems, e.g. when the system has two or more unmeasured external contact wrenches. It is based on inverse dynamics and a quadratic optimization, and is therefore relatively simple, computationally cost effective and robust. Net joint loads (NJLs) are included as variables of the problem, and thus could be estimated in the same procedure as the ECL and be used within the cost function.

The proposed method is tested on human sit-to-stand maneuvers performed holding a handle with one hand, i.e. asymmetrical movements with multiples external contacts. Three sets of measured and unmeasured contact load components and three cost functions are considered and simulated results are compared to experimental data. For the population and movement studied, better results are obtained for a least-square sharing between actuated degrees-of-freedom of the relative motor torques (motor torques normalized by the maximal torque production capacity). Moreover, the number of unknown ECL components does not significantly influence the results. In particular, measuring only the vertical force under the seat lead to a relatively correct estimation of the ECL and NJT: not only the values of $R_{\%}$ were small (about 10% for the feet ECL and 20% for the NJT), but the influence of an experimental parameters (the Seat Height) was also correctly predicted.

1. Introduction

Human motion analysis focuses more and more on dynamic variables. In particular, analysis of the external contact loads (ECL) allows characterizing the nature and the role of interactions between a subject and its environment. For example, Chateauroux and Wang (2010) classified hand/vehicle contacts during car ingress/egress motions based on their role on the motion: exploration of the environment, balance maintenance and participation to the displacement.

Knowledge of the ECL is also necessary to analyze the dynamics of a motion, typically the internal loads such as the net joint torques (NJT) or muscle forces. These internal loads are not directly measurable with non-invasive techniques. They are usually estimated using inverse dynamic approaches, i.e. based on the knowledge of the system's kinematics, its inertia properties and the ECL acting on it (e.g. Dariush et al., 2000; Doriot and Cheze, 2004; Dumas et al., 2007b; Silva and Ambrósio, 2002; Winter, 1990).

Classically, ECL are directly recorded using load sensors. However, direct measurement may be technically complex, especially for ambulatory or "out of the lab" experiments. Besides, use of force sensors tends to reduce the "ecological" aspect of an experiment. A classical illustration would be the force plate targeting problem in gait analyses (Challis, 2001; Oggero et al., 1998). Another example would be ergonomic experiments performed in complex environments, such as car ingress–egress (Causse et al., 2009; Kim and Lee, 2009) where the difficulty to equip every mock-up parts lead experimenters to limit the possible contact areas for the subject, and eventually limit the variety and naturalness of movements.

Therefore, it is necessary to use modeling techniques to indirectly estimate the ECL from the known kinematics of body segments (measured or simulated). One of the method could be to use a detailed model of the contacts, in particular for the foot-ground contact during locomotion (Fluit et al., 2012; Pandy, 2001). However, such models are difficult to adjust, potentially expensive in computation and sensitive to the modeling hypotheses (Dorn et al., 2012).

* Corresponding author at: Université de Lyon, F-69622, Lyon, France. Tel.: +33 4 72 14 23 93.
E-mail address: thomas.robert@ifsttar.fr (T. Robert).

0021-9290/$ - see front matter © 2013 Elsevier Ltd. All rights reserved.
http://dx.doi.org/10.1016/j.jbiomech.2013.06.037

An alternative is to use an inverse approach, i.e. to estimate the ECL acting on a system that lead to its observed motion (Pillet et al., 2010; Sanders and Wilson, 1991). However, one of the limitations of this approach is that it becomes underdetermined if there are more unknown ECL components than independent governing equations. This usually occurs when there are multiple unmeasured contacts loads with the environment. Thus, setting an assumption on the load sharing becomes necessary.

In the past, only few studies have proposed to deal with these types of underdetermined problems. Most of them focused on bipedal phase of the gait and represented the load sharing with mathematical functions (Davis and Cavanagh, 1993; Hardt and Mann, 1980; Koopman et al., 1995; Ren et al., 2008). While these methods provided satisfying results, they were very specific to the given task and the population. A more generic approach for solving the load sharing problem consists by minimizing a cost function was presented by (Vaughan et al., 1982). Instead of focusing only on the ECL problem, Vaughan et al. (1982) chose to explicitly introduce the unknown net joint loads (NJL) into the problem. It allowed to estimate NJL and ECL in the same procedure and also to use NJL into the cost function. Based on this approach, they obtained interesting results for different kind of movements. However, the study suffered from several limitation: there results were strongly dependent on the initial guess of the solution, the methods was only tested in 2D and in cases with no more than two unknown ECL wrenches, and the results were reported for only one cost function.

This indicates that there is still a lack of methodologies for estimating the ECL, particularly in underdetermined cases. This study proposes a generic method which utilizes a combination of inverse dynamics and optimization. It is intended to be relatively simple, computationally cost effective and robust. The proposed method is tested on human sit-to-stand maneuvers performed holding a handle with one hand, i.e. asymmetrical movements with multiples external contacts. Influence of the number of unknown ECL components and of different cost functions are evaluated.

2. Modeling

This section introduces the generic problem to be solved in this study.

2.1. Description of system considered

The system considered is a whole body human model made of n_s rigid segments linked by n_j joints representing a total of n_{dof} degrees-of-freedom (DoF). The kinematics and inertia properties of the segments are considered to be known.

2.2. Dynamics and constraints of the system

The dynamic wrenches for each segment, due to the inertial and gravitational effects, can be estimated from its kinematics and inertia properties. This wrench has to be balanced by the unknown external loads acting on this segment (applied by the neighboring segments (NJL) and by external contacts (ECL)). It leads to 6 linear Newton–Euler equations per segment. Based on the topology of the model, we can write them for every segments. It results in a set of $6n_s$ linear equations (6 per segments) with $n_u + 6n_j$ unknowns (corresponding to the unknown ECL components and the NJL)

$$a_{eq}x = b_{eq} \tag{1}$$

where $x = [S\ U]^t$ is a single vector grouping all the unknowns, S is the vectors containing the $6n_j$ NJL (3 forces and 3 torques per joint), U is the vectors of the n_u unknown ECL components, a_{eq} is a matrix relating the joints and unknown ECL components with the corresponding affected segments, and b_{eq} is the effect of the dynamic wrench, known ECL and loads due to the gravity for all the segments (see Appendix for the details).

The physical limitations of the studied system, such as unilaterality of the contacts, non-sliding of the contact points, or maximum motor torques that could be developed, are also considered in this study. In order to make the resolution of the problem faster and more robust (see Section 2.3), we chose to express these limitations as linear equations of the unknown vector x. Mathematical description of these constraints are given in Appendix.

The description of the system dynamics and limitations boils down to the linear system

$$\begin{cases} a_{eq}x = b_{eq} \\ a_c x \le b_c \end{cases} \tag{2}$$

2.3. Resolution

This study focuses on underdetermined problems for which there are fewer governing equations than the unknowns ($6n_s < 6n_j + n_u$). In order to select only one solution among all the possibles, additional expectations for this solution are introduced via a function to be minimized. For numerical purposes (developed in the discussion) we propose: (1) to write this function in a specific form (squared euclidean norm of a linear function of x), (2) to add an additional term to it—the squared euclidean norm of x with a very low weighting factor—and (3) to set the equality constraints as penalties. Eventually, it led to the following optimization problem:

$$\min_x \alpha\|sx\|^2 + \beta\|x\|^2 + \gamma\|a_{eq}x - b_{eq}\|^2 \quad \text{s.t. } a_c x \le b_c \tag{3}$$

where $\|\|$ represents the euclidean norm, s is a matrix defining a linear transformation of x, and α, β and γ are weighting factors.

This problem can be rewritten as a quadratic programming problem

$$\min_x \frac{1}{2}x^T H x + g^T x \quad \text{s.t. } a_c x \le b_c \tag{4}$$

with $H = 2\alpha s^T s + \beta I + \gamma a_{eq}^T a_{eq}$ a positive definite matrix (see Discussion) and $g^T = -2\gamma b_{eq}^T a_{eq}$.

3. Case study

3.1. Task and motions studied

Experimental data were collected on six healthy young male volunteers (stature = 1752 ± 61 mm, weight = 66 ± 8 kg and age = 26 ± 3 yo), having no musculoskeletal disorder.

Subjects were initially seated on a flat rigid seat with feet on the ground and the right hand grasping a horizontal handle. The handle was centered in the sagittal plane of the subject, located at the level of the subject's eyes when seated and at a distance corresponding to the shoulder-wrist length. They were asked to rise from the seat to a standing posture using the handle (see Fig. 1). Three different seat heights were tested: 50% (H_{50}), 75% (H_{75}) or 100% (H_{100}) of the knee height. The task was repeated two times for H_{50} and H_{100} and six times for H_{75}.

3.2. Experimental data collection and processing

A Motion Analysis® system, sampling at 100 Hz, was used to capture the trajectories of 51 reflective markers placed on the subject. All ECL between the subject and its environment were recorded using

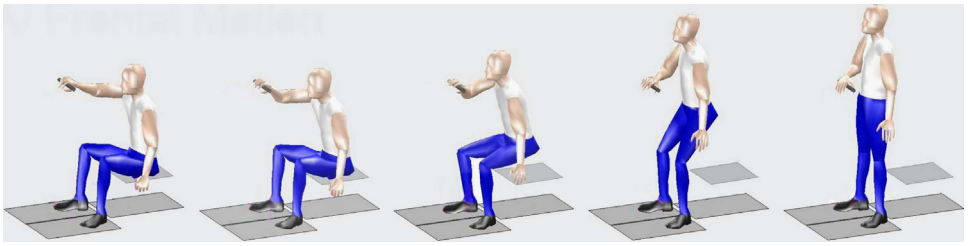

Fig. 1. The sit-to-stand maneuver considered: example of a reconstructed motion with the seat height at 75% of the knee height.

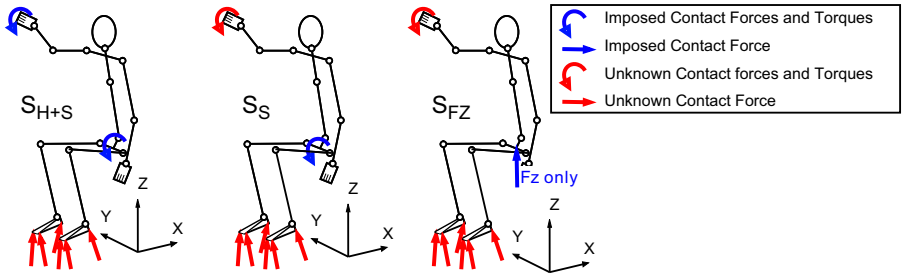

Fig. 2. The multibody model considered in the three contact configurations tested. Straight and curved arrows stand for forces and full wrench respectively, whereas blue and red colors stand for known and unknown contact loads respectively. (For interpretation of the references to color in this figure caption, the reader is referred to the web version of this paper.)

three force plates (under each foot and under the seat) and a 6-axes load sensor placed between the handle and the frame.

Kinematics was reconstructed using a global optimization procedure and a kinematic model fitted to the subject's anthropometry (Wang et al., 2005). This model (see Fig. 2) is made of 16 rigid bodies (feet, lower limbs, thighs, pelvis, abdomen, thorax, head & neck, arms, forearms and hands) linked by 15 joints and 37 degrees-of-freedom (see Table 1). For each subject, the inertia parameters of these 16 segments were estimated from regression equations based on body weight and segment lengths (Dumas et al., 2007a). NJL were computed using a recursive approach (Doriot and Cheze, 2004) and two calculation strategies (bottom-up and top-down) converging at the lumbar joint (Robert et al., 2007). These NJL computed using all the contact loads information will later be used as reference to estimate the quality of the optimization (see Section 3.5).

3.3. Modeling hypotheses

The methodology proposed in Section 2 is applied using the measured kinematics and different subsets of the measured ECL.

Three different sets of known (i.e. which are measured) and unknown ECL were considered (see Fig. 2): (1) S_{H+S}—both seat and hand contact wrenches are known; (2) S_S—only seat contact wrench is known; (3) S_{F_Z}—only the vertical force of seat contact wrench is known and other components are assumed absent. When unknown, hand to handle interaction was represented by a full wrench applied at the projection of the third metacarpophalangeal joint on the handle. The contact between the foot and the ground were modeled as 3 punctual unilateral contacts with tangential force limited by friction (static coefficient $\mu = 0.5$) and positioned under the 1st and the 5th metatarsal heads and the heel. These 3 punctual contact wrenches were further aggregated to represent the foot to ground interaction with a single contact wrench.

Three types of constraints were applied: unilaterality and dry friction constraints for punctual contacts, and maximal motor torques that could be developed by the subject (see Table 1). Mathematical description of these constraints are given in Appendix.

3.4. Resolution of the optimization problem

Three different expectations on the load sharing were tested: minimization in a least-square sense of (1) the unknown external contact forces (ECF)(C_{ECF}); (2) the net joint torques (NJT)(C_{NJT}), (3) the motor torques normalized by their maximum allowable value ($MT_{\%}$ see Table 1) $C_{MT_{\%}}$. It resulted in three cost functions C_i's of the form

$$C_i(x) = \alpha_i \|s_i x\|^2 + \beta \|x\|^2 + \gamma \|a_{eq} x - b_{eq}\|^2 \quad (5)$$

with s_i matrices defining the linear transformation of x—the unknown vector of ECL and NJL—into the vector of ECF, NJT or $MT_{\%}$ respectively (details in Appendix). Values of α_i were adjusted based on the average value of s_i (see Table 2), while β and γ were set to 10^{-5} and 10^{5} respectively.

These quadratic programming problems were solved using the Matlab® *quadprog* solver, based on an deterministic interior-point method. The algorithm was automatically initialized for the first frame of the motion (initial point set to a vectors of ones MathWorks, 2012). For the remaining frames it was initialized using the results of the previous frame.

3.5. Analyses

Three cost functions (C_{ECF}, C_{NJT}, $C_{MT_{\%}}$), three contact configurations (S_{H+S}, S_S, S_{F_Z}) and three experimental seat heights (H_{50}, H_{75} and H_{100}) were considered. Seven combinations of these variables were tested (see Table 2). For each of them, the NJL and the unknown ECL were estimated for every maneuver performed by the six subjects. Forces and torques were normalized by body weight (BW) and body weight times body height (BW × BH) respectively (Hof, 1996). Peak values of the norm of the simulated ECL and NJT were extracted and referred as P_{sim} hereafter. In addition, time history profiles of the norm of the simulated data were compared to their reference curves using RMS differences (R). They were further normalized by the amplitude of the reference curve and referred as $R_{\%}$. The reference data were: (1) the measured experimental data for the ECL; (2) the results of the inverse dynamics performed using the experimentally measured ECL (see Section 3.2) for the NJT.

Table 1
List of joints and their associated degrees-of-freedom and maximum torques for the considered model.

Joint	Motion	Max torque (N m)	Source
Hip joint	Flexion	185	Chaffin et al. (2006)
	Extension	190	Chaffin et al. (2006)
	Abduction	190	Delp (1990)
	Adduction	190	Delp (1990)
	Internal rotation	60	Delp (1990)
	External rotation	60	Delp (1990)
Knee joint	Flexion	100	Chaffin et al. (2006)
	Extension	168	Chaffin et al. (2006)
	Internal rotation	20	Expertize
	External rotation	20	Expertize
Ankle joint	Dorsiflexion	126	Chaffin et al. (2006)
	Plantarflexion	126	Chaffin et al. (2006)
	Inversion	20	Expertize
	Eversion	20	Expertize
Shoulder joint	Flexion	92	Chaffin et al. (2006)
	Extension	67	Chaffin et al. (2006)
	Abduction	71	Chaffin et al. (2006)
	Adduction	67	Chaffin et al. (2006)
	Internal rotation	52	Chaffin et al. (2006)
	External rotation	33	Chaffin et al. (2006)
Elbow joint	Flexion	77	Chaffin et al. (2006)
	Extension	46	Chaffin et al. (2006)
	Pronation	15	Garner and Pandy (2000)
	Supination	15	Garner and Pandy (2000)
Wrist joint	Flexion	185	Garner and Pandy (2000)
	Extension	190	Garner and Pandy (2000)
	Abduction	190	Garner and Pandy (2000)
	Adduction	190	Garner and Pandy (2000)
Lumbar joint	Flexion	143	Chaffin et al. (2006)
	Extension	234	Chaffin et al. (2006)
	Right bending	159	Chaffin et al. (2006)
	Left bending	159	Chaffin et al. (2006)
	Left axial rotation	∅	
	Right axial rotation	∅	
Thoracic joint	Flexion	∅	
	Extension	∅	
	Right bending	∅	
	Left bending	∅	
	Left axial rotation	∅	
	Right axial rotation	∅	
Neck joint	Flexion	100	Chaffin et al. (2006)
	Extension	100	Chaffin et al. (2006)
	Right bending	∅	
	Left bending	∅	
	Left axial rotation	∅	
	Right axial rotation	∅	

ANOVAs and Tukey's post-hoc tests were used to analyze the effects of (1) the cost function on $R_{\%}$ in S_S and H_{75} (three first rows of Table 2), (2) the contact configuration on $R_{\%}$ using $C_{MT_{\%}}$ and in H_{75} (rows three to six of Table 2), and (3) the seat height on P_{sim} using $C_{MT_{\%}}$ and in S_{F_Z} (last three rows of Table 2).

4. Results

The procedure successfully converged for all the tested motions and configurations. An evaluation was performed to observe if equality constraints set as penalties were satisfied. It was found that the residual values of $\|a_{eq}.x-b_{eq}\|^2$ (see Eq. (5)) remained negligible (less than 10^{-4}) in all cases, except for some motions in contact the configuration S_{H+S}, where it reached up to 3 N m around the seat-off for torque constraints along the transverse axis.

Fig. 3 displays an example of reference data (measured ECL and NJT obtained through inverse dynamics with the measured ECL) for a representative subject in configuration S_S and H_{75}. Loads are expressed in coordinate systems parallel to the Global Coordinate System (displayed in Fig. 2) and centered at the joint considered.

Table 2
The different combination of parameters tested, and the corresponding weights of the cost function.

#	Cost function	Contact configuration	Seat height	α_i	β	γ	Tested effect
1	C_{ECF}	S_S	H_{75}	10^{-1}	10^{-5}	10^5	Cost function
2	C_{NJT}	S_S	H_{75}	1	10^{-5}	10^5	
3	$C_{MT_{\%}}$	S_S	H_{75}	500	10^{-5}	10^5	
4	$C_{MT_{\%}}$	S_{H+S}	H_{75}	500	10^{-5}	10^5	Contact configuration
3	$C_{MT_{\%}}$	S_S	H^{75}	500	10^{-5}	10^5	
5	$C_{MT_{\%}}$	S_{F_Z}	H_{75}	500	10^{-5}	10^5	
6	$C_{MT_{\%}}$	S_{F_Z}	H_{50}	500	10^{-5}	10^5	Seat height
5	$C_{MT_{\%}}$	S_{F_Z}	H_{75}	500	10^{-5}	10^5	
7	$C_{MT_{\%}}$	S_{F_Z}	H_{100}	500	10^{-5}	10^5	

These results are comparable in term of profiles and amplitude to the classical data available in the literature for sit-to-stand maneuvers (Bahrami et al., 2000; O'Meara and Smith, 2006). In this Fig. 3, simulated results obtained in the same situation for different cost functions are also superimposed to the reference data. Both the shape of the simulated curves and their amplitudes are overall in good agreement with the reference ones.

An example of simulated and measured center of pressure trajectories under each foot is shown in Fig. 4. The loaded area are comparable. In this particular case the experimental trajectory goes outside the modeled base of support (BoS) for some frames of the motion, whereas the simulated trajectory remains inside.

Table 3 displays the value of RMS differences between the simulated and reference data (R) averaged across trials and subjects for each contact and joints and the three cost functions tested (contact configuration S_S and seat height H_{75}). The normalized RMS ($R_{\%}$) are plotted in Fig. 5. Very high values for the right wrist NJT are due to very small amplitudes of the reference curves. Therefore, they are discarded in further analyses. Overall, $R_{\%}$ are smaller for $C_{MT_{\%}}$ and higher for C_{ECF}. This is confirmed by an ANOVA with factors *Contact* and *Cost function* performed on the $R_{\%}$ values of the ECF. It showed a significant effect ($p<0.05$) of the *Cost function*, the *Contact* and their interactions. Post-hoc tests showed that $R_{\%}$ are significantly different for each cost function, with the smallest values for $C_{MT_{\%}}$ and the highest for C_{ECF}. Similar results are obtained for the NJT, although $R_{\%}$ for C_{NJT} and $C_{MT_{\%}}$ are not significantly different.

A similar analysis was performed to evaluate the effect of the contact configuration using the cost function $C_{MT_{\%}}$ in seat height H_{75}. An ANOVA with factors *Contact* and *Contact configuration* performed on the $R_{\%}$ for the ECF showed that neither the *Contact configuration* nor the interaction has a significant effect ($p=0.157$ and $p=0.321$, respectively). Similar results are obtained for the NJT.

Two ANOVAs with factors *Contact* and *Seat height* performed on the P_{sim} for the ECF and for the NJT confirmed that the *Seat height* has a significant effect on the P_{sim}. Post-hoc tests showed that the higher the seat the smaller the P_{sim} ($H_{100}<H_{75}<H_{50}$).

5. Discussion

5.1. Quality of the results

This paper presents a general method to estimate unmeasured external contact loads acting on a system whose kinematics and inertial properties are known. The proposed method is applied to sit-to-stand motions with a handle. The normalized RMS differences between simulated and reference data ($R_{\%}$) are relatively small, in particular for the cost function $C_{MT_{\%}}$: about 10% for the feet ECL and 20% for the NJT. These values are comparable with

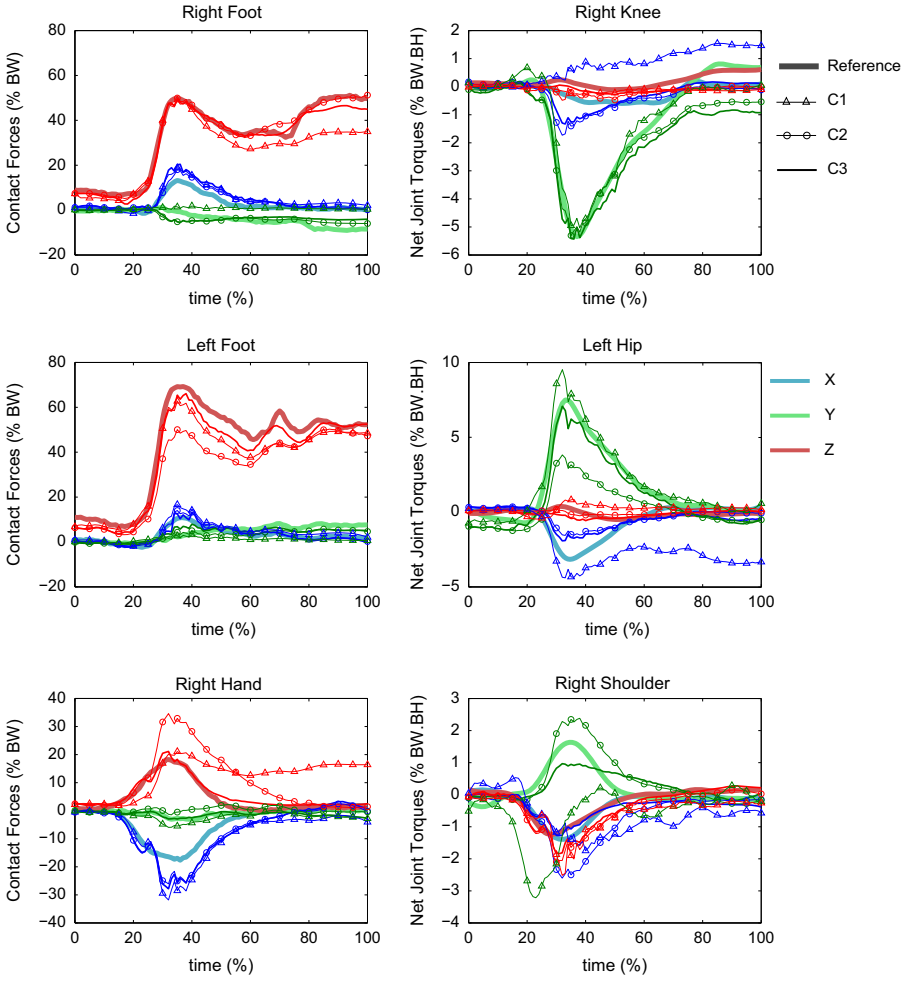

Fig. 3. Example of reference and simulated contact forces and joint torques obtained for a sit-to-stand motion (seat height at 75% of the knee height, contact configuration *S2*) for three different cost functions. Data are expressed in coordinate systems parallel to the Global Coordinate System (see Fig. 2). Differences among the cost functions are best seen for hand forces and shoulder torques (see last row in the figure).

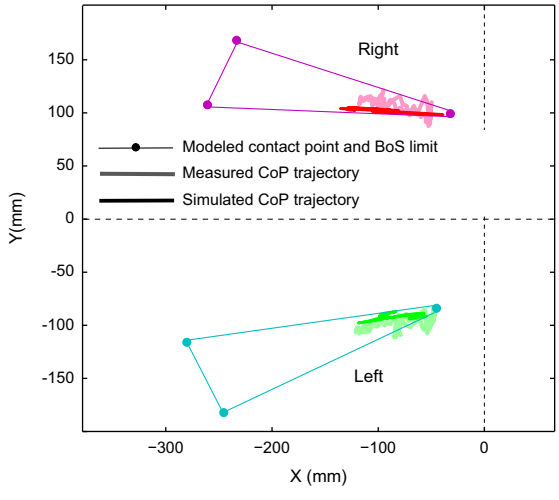

Fig. 4. An example of the measured and simulated trajectories of the Center of Pressure under each foot, expressed in the global coordinate system (see Fig. 2). Note that in this case the experimental trajectories goes out of the modeled base of support, while the simulated trajectories remain inside.

Table 3
RMS differences between simulated and reference data—see Section 3.5)—averaged across subjects and trials, in contact configuration S_S and seat height H_{75}. Values are expressed in percentage of Body Weight for the contact forces and percentage of Body Weight time Body Height for the joint torques.

		C_{ECF}	C_{NJT}	$C_{MT_{75}}$
Contact forces (RMS in % of BW)	Left foot	8.62	10.85	5.18
	Right foot	5.59	8.15	5.47
	Right hand	7.51	4.53	3.97
Net joint torques (RMS in % of BW*BH)	Left ankle	0.46	0.40	0.44
	Left knee	0.82	0.58	0.70
	Left hip	1.23	1.31	0.75
	Right ankle	0.70	1.01	1.07
	Right knee	0.81	1.04	1.06
	Right hip	0.93	0.77	1.09
	Lumbar	1.64	2.03	1.52
	Right shoulder	1.50	0.50	0.38
	Right elbow	2.75	1.19	0.48
	Right wrist	2.06	0.48	0.12

those obtained by Ren et al. (2008) for a similar problem (estimation of the ECL and NJT during a gait cycle without using the measured ground reaction forces) but with a method very specific to the studied motion. Moreover, $R_{\%}$ values are of the same order as the possible errors of a classical whole body inverse dynamics estimated experimentally by Causse et al. (2009) or from simulation by Riemer et al. (2008).

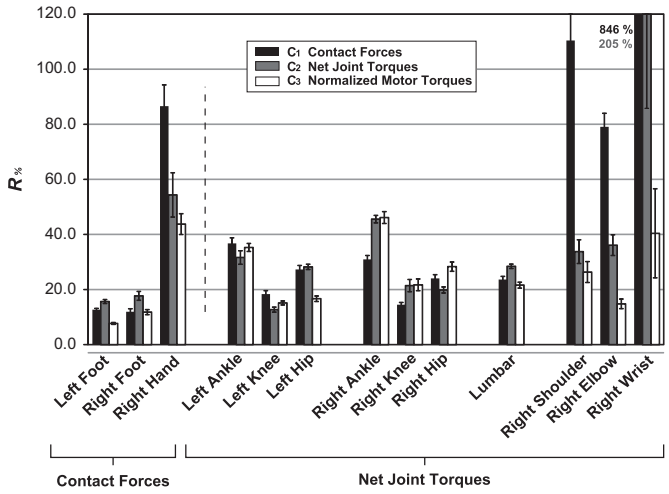

Fig. 5. $R_{\%}$ (normalized RMS differences between simulated and reference data—see Section 3.5) for different cost functions and different joint and contacts, averaged across subjects and trials, in contact configuration S_S and seat height H_{75}. Vertical bars represents $\pm$ one standard error of the mean (SEM). Results above 120% are given in the figure. The high values for the right wrist net joint torques are due to small amplitudes of the experimental curves.

5.2. Numerical aspects

This method is intended to be relatively simple and robust. For the case study considered the optimization problem converges systematically, and one could remark the smoothness of the time profile for the simulated variables, although the problem is solved frame by frame. It is notably imputable to the numerical properties of the optimization problem. We choose to write the problem as a quadratic program (quadratic cost function and linear constraints), which are a class of convex optimization problems (Boyd and Vandenberghe, 2004). For this type of problem, if the H matrix of the cost function (see Eq. (5)) is positive definite (always non-negative, nil only for $x=0$) and if the problem has a solution, then this solution is a global minimum and is unique. Thus, the solver systematically and quickly converges toward this desired solution.

The cost functions used in this study are the sum of three terms (see Eq. (5)). The first and last terms are strictly non-negative functions that may be equal to zero for non-zero value of x. Adding the squared norm of x, even with a very small weight, ensures that the cost function can only be nil only when $x=0$, i.e. the cost functions are positive definite. In other words, the first and last terms of the cost function do not necessarily nullify the space of solution. Typically the foot contact model used in this study (3 contact points) induces a redundancy in the horizontal plane: an infinity of individual contact forces combinations result in the same overall contact force for the foot, and thus the same motor torques and the same value of the optimization criterion. The role of the second part of the criterion, slightly weighted, is then to nullify the space of solution and as such to improve the stability and convergence efficiency of the optimization algorithm. Because of its small relative weight, it does not significantly change the results in terms of the resultant of ECL or NJL.

This study focuses on underdetermined problems. However, in some situations, the system of Eq. (2) may become over-constrained. It typically happens in case of temporary inconsistencies between the modeling hypotheses and the imposed experimental data (estimated accelerations or BSIP). In this study we choose to set the equality constraints as penalties in the cost function. It lead to the optimization problem (3), only constrained by the set of inequalities representing the system's limitations. These later are independent of the experimental data and, besides modeling incoherences, unlikely to nullify the space of solution. Consequently, the problem (3) always has at least a solution. Although this solution only satisfies as well as possible the equations of motion, it may be acceptable for small residual values of the penalties. In this study over-constrained situations may happen around the seat-off in the contact configuration S_{H+S}. As displayed in Fig. 4, the foot contact wrenches may be too tightly constrained for some motion, leading to small discrepancies between the modeled BoS and the experimental CoP trajectory. These discrepancies could be compensated by the hand contact wrench when this later is not imposed, but lead to an over-constrained problem when the hand contact wrench is imposed (contact configuration S_{H+S}). The observed residual values remain relatively small, and the obtained solutions are thus acceptable. However, a track for improvement would be to finely define the shape of the BoS, by adding contact points for example.

In this study, the system's dynamics is described without explicitly considering the kinematic constraints on the joints, i.e. using a Newton–Euler formalism rather than a Lagrangian formalism. Note however that the kinematic constraints are implicitly introduced by the segment kinematics, obtained via a global optimization procedure based on a kinematic model. Also, the NJL are further transformed into the actuating forces (motor torques), using this kinematic model. Although this choice increases the size of the optimization problem (the number of unknowns), it does not increase its degree of indeterminacy (each "unnecessary" unknown is supported by an additional equation).

5.3. Case study: cost functions, contact configurations and applicability

Different load sharing hypotheses are tested. Cost function $C_{MT_{\%}}$ provides the better results (the smaller $R_{\%}$). It principally implies a least-square sharing between actuated DoF of the relative motor torques (motor torques normalized by the maximal torque production capacity). It therefore prevents to overload those DoF which are having small capacity. This effect is best seen on the right upper limb, where the use of $C_{MT_{\%}}$ tends to limit the loads along the right upper limb DoF, with smaller force production capacities relative to those of the lower limbs. This criterion is quite similar to the minimization of the individual muscle stress (individual muscle forces normalized by their physiological cross-sectional area) classically used for solving the underdetermined muscle force sharing problem (e.g. Erdemir et al., 2007, for a review). Other criteria could be considered, in particular the p-norm of s_{ix} to the power p with $p\neq 2$ and the min/max criterion (Rasmussen et al., 2001). Also, it could be interesting to include individual muscle forces in the criterion. It would not change the nature of the problem as, by neglecting the contraction dynamics, the muscle forces can be expressed as a linear function transformation of the motor torques via a level arm matrix.

Three different contact configurations are considered in this study. Statistical analysis shows that this parameter do not significantly influence the quality of the results (difference between reference and simulated data). In particular, reducing the number of unknowns do not improve the $R_{\%}$ (S_{H+S} vs S_S). It is also remarkable that the quality of the results remains correct, even when none of the external forces acting on the system were specified (after the seat-off in contact configurations S_S and S_{F_Z}).

Results obtained in the S_{F_Z} contact configuration (using only the vertical force component of the seat contact wrench) are particularly interesting in terms of application. They suggest that, for the studied movement and population, measuring only the vertical force under the seat allows a relatively correct estimation of all ECL and NJT: not only the values of $R_{\%}$ are small, but the influence of an experimental parameter (the Seat Height) is also correctly predicted. In this case,

peak values of NJT and ECL increases when the seat height decreases, as observed from the experimental data (Robert et al., 2011). This could be of particular importance for ergonomic studies where usually the goal is to understand the influence of different experimental parameters on the motion dynamics and which often suffer from instrumentation difficulties.

5.4. Limitations

The methodology is only evaluated for one type of motion and a small sample of single population. Load sharing criterion may evolve between motion and population, and may include other parameters such as the comfort or balance. This should be further studied.

Another limitation comes from the fact that maximal torque production capacities are set as constants (see Table 1), although they depend of several factors such as the subject or the posture. It may primarily affect the load sharing for the $C_{MT_{\%}}$ cost function (maximal values being not reached in the studied motion). A track to overcome this limitation could be the use of muskuloskeletal models, notably for their capacity to represent the relations between maximum torque and joint angle (e.g. Delp and Zajac, 1992). However, a detailed personalization of such models remains a challenge (Fregly et al., 2012).

Moreover, the contact configurations considered in this study remains constant during the motion. Although the kinematics and measured contact loads may sufficiently drive the problem, discontinuities in solution may appear when considering intermittent contacts. One could thus consider describing the problem using parametric curves and solving it as a whole instead of frame by frame (e.g. Seguin et al., 2005). In addition, this method, based on rigid body modeling, performs well with relatively simple contacts such as the hand/handle or foot/ground interactions. However, including more complex deformable contacts such as the seat buttock interactions into the ECL estimation would require further investigations.

Lastly, it is important to remind that, as for a classical inverse dynamic procedure, the accuracy of the results depends on the quality of the inputs, and in particular the reconstructed kinematics, inertia parameters and point of force application of the known contact forces (Rao et al., 2006; Ren et al., 2008; Silva and Ambrósio, 2004).

Conflict of interest statement

Authors have no conflict of interest to report in this research.

Appendix A. Supplementary material

Supplementary data associated with this article can be found in the online version at http://dx.doi.org.10.1016/j.jbiomech.2013.06.037.

References

Bahrami, F., Riener, R., Jabedar-Maralani, P., Schmidt, G., 2000. Biomechanical analysis of sit-to-stand transfer in healthy and paraplegic subjects. Clinical Biomechanics 15, 123–133.

Boyd, S., Vandenberghe, L., 2004. Convex Optimization. Cambridge University Press.

Causse, J., Chateauroux, E., Monnier, G., Wang, X., Denninger, L., 2009. Dynamic analysis of car ingress/egress movement: an experimental protocol and preliminary results. SAE International Journal of Passenger Cars-Mechanical Systems 2, 1633–1640.

Chaffin, D., Andersson, G., Martin, B., 2006. Occupational Biomechanics, 4th ed. John Wiley & Sons, New York, NY.

Challis, J.H., 2001. The variability in running gait caused by force plate targeting. Journal of Applied Biomechanics 17, 77–83.

Chateauroux, E., Wang, X., 2010. Car egress analysis of younger and older drivers for motion simulation. Applied Ergonomics 42, 169–177.

Dariush, B., Hemami, H., Parnianpour, M., 2000. A well-posed, embedded constraint representation of joint moments from kinesiological measurements. Journal of Biomechanical Engineering 122, 437–445.

Davis, B.L., Cavanagh, P.R., 1993. Decomposition of superimposed ground reaction forces into left and right force profiles. Journal of Biomechanics 26, 593–597.

Delp, S., Zajac, F.E., 1992. Force- and moment-generating capacity of lower-extremity muscles before and after tendon lengthening. Clinical Orthopaedics and Related Research 284, 247–259.

Delp, S.L., 1990. Surgery Simulation: A Computer Graphics System to Analyze and Design Musculoskeletal Reconstructions of the Lower Limb. Ph.D. Thesis. Stanford University.

Doriot, N., Cheze, L., 2004. A three-dimensional kinematic and dynamic study of the lower limb during the stance phase of gait using an homogeneous matrix approach. IEEE Transactions on Biomedical Engineering 51, 21–27.

Dorn, T.W., Lin, Y.C., Pandy, M.G., 2012. Estimates of muscle function in human gait depend on how foot-ground contact is modelled. Computer Methods in Biomechanics and Biomedical Engineering 15, 657–668.

Dumas, R., Cheze, L., Verriest, J.P., 2007a. Adjustments to Mcconville et al. and Young et al. body segment inertial parameters. Journal of Biomechanics 40, 543–553.

Dumas, R., Nicol, E., Cheze, L., 2007b. Influence of the 3D inverse dynamic method on the joint forces and moments during gait. Journal of Biomechanical Engineering 129, 786–790.

Erdemir, A., McLean, S., Herzog, W., van den Bogert, A.J., 2007. Model-based estimation of muscle forces exerted during movements. Clinical Biomechanics (Bristol, Avon) 22, 131–154.

Fluit, R., van der Krogt, M., van der Kooij, H., Verdonschot, N., Koopman, H., 2012. A simple controller for the prediction of three-dimensional gait. Journal of Biomechanics 45, 2610–2617.

Fregly, B., Boninger, M., Reinkensmeyer, D., 2012. Personalized neuromusculoskeletal modeling to improve treatment of mobility impairments: a perspective from European research sites. Journal of NeuroEngineering and Rehabilitation 9, 18.

Garner, B., Pandy, M., 2000. Musculoskeletal model of the upper limb based on the visible human male dataset. Computer Methods in Biomechanics and Biomedical Engineering 4, 93–126.

Hardt, D.E., Mann, R.W., 1980. A five body—three dimensional dynamic analysis of walking. Journal of Biomechanics 13, 455–457.

Hof, A.L., 1996. Scaling gait data to body size. Gait & Posture 4, 222–223.

Kim, S., Lee, K., 2009. Development of discomfort evaluation method for car ingress motion. International Journal of Automotive Technology 10, 619–627.

Koopman, B., Grootenboer, H.J., de Jongh, H.J., 1995. An inverse dynamics model for the analysis, reconstruction and prediction of bipedal walking. Journal of Biomechanics 28, 1369–1376.

MathWorks, 2012. Optimization Toolbox User's Guide, Matlab R2012b.

Oggero, E., Pagnacco, G., Morr, D., Simon, S., Berme, N., 1998. Probability of valid gait data acquisition using currently available force plates. Biomedical Sciences Instrumentation 34, 392–397.

O'Meara, D.M., Smith, R.M., 2006. The effects of unilateral grab rail assistance on the sit-to-stand performance of older aged adults. Human Movement Science 25, 257–274.

Pandy, M., 2001. Computer modeling and simulation of human movement. Annual Review of Biomedical Engineering 3, 245–273.

Pillet, H., Bonnet, X., Lavaste, F., Skalli, W., 2010. Evaluation of force plate-less estimation of the trajectory of the centre of pressure during gait. Comparison of two anthropometric models. Gait & Posture 31, 147–152.

Rao, G., Amarantini, D., Berton, E., Favier, D., 2006. Influence of body segments' parameters estimation models on inverse dynamics solutions during gait. Journal of Biomechanics 39, 1531–1536.

Rasmussen, J., Damsgaard, M., Voigt, M., 2001. Muscle recruitment by the min/max criterion—a comparative numerical study. Journal of Biomechanics 34, 409–415.

Ren, L., Jones, R.K., Howard, D., 2008. Whole body inverse dynamics over a complete gait cycle based only on measured kinematics. Journal of Biomechanics 41, 2750–2759.

Riemer, R., Hsiao-Wecksler, E.T., Zhang, X., 2008. Uncertainties in inverse dynamics solutions: a comprehensive analysis and an application to gait. Gait & Posture 27, 578–588.

Robert, T., Causse, J., Wang, X., 2011. Dynamics of sit-to-stand motions: effect of seat height, handle use and asymmetrical motions. Computer Methods in Biomechanics and Biomedical Engineering 14 (Suppl 1), 191–192.

Robert, T., Chèze, L., Dumas, R., Verriest, J.P., 2007. Validation of net joint loads calculated by inverse dynamics in case of complex movements: application to balance recovery movements. Journal of Biomechanics 40, 2450–2456.

Sanders, R.H., Wilson, R.K., 1991. Accuracy of derived ground reaction force curves for a rigid link human body model. Journal of Applied Biomechanics 7, 330–343.

Seguin, P., Bessonnet, G., Sardain, P., 2005. A parametric optimization approach to walking pattern synthesis. International Journal of Robotics Research (IJRR) 24, 523–536.

Silva, M., Ambrósio, J., 2002. Kinematic data consistency in the inverse dynamic analysis of biomechanical systems. Multibody System Dynamics 8, 219–239.

Silva, M.P., Ambrósio, J.A., 2004. Sensitivity of the results produced by the inverse dynamic analysis of a human stride to perturbed input data. Gait & Posture 19, 35–49.

Vaughan, C.L., Hay, J.G., Andrews, J.G., 1982. Closed loop problems in biomechanics. Part II—an optimization approach. Journal of Biomechanics 15, 201–210.
Wang, X., Chevalot, N., Monnier, G., Ausejo, S., Ángel, Suescun, Celigüeta, J., 2005. Validation of a model-based motion reconstruction method developed in the realman project. SAE Transactions Journal of Passenger Cars – Electronic and Electrical Systems 114, 873–879.
Winter, D., 1990. Biomechanics and Motor Control of Human Movement. John Wiley & Sons, New York, NY.